Time-resolved electronic capture in *n*-type germanium doped with antimony

N. Deßmann,[1] S. G. Pavlov,[2] V. N. Shastin,[3,4] R. Kh. Zhukavin,[3] V. V. Tsyplenkov,[3] S. Winnerl,[5] M. Mittendorff,[5,6] N. V. Abrosimov,[7] H. Riemann,[7] and H.-W. Hübers[1,2]

[1]*Institut für Optik und Atomare Physik, Technische Universität Berlin, Berlin, Germany*
[2]*Institute of Planetary Research, German Aerospace Center (DLR), Berlin, Germany*
[3]*Institute for Physics of Microstructures, Russian Academy of Sciences, Nizhny Novgorod, Russia*
[4]*Nizhny Novgorod State University, Nizhny Novgorod, Russia*
[5]*Helmholtz-Zentrum Dresden-Rossendorf, Dresden, Germany*
[6]*Technische Universität Dresden, Dresden, Germany*
[7]*Leibniz Institute for Crystal Growth, Berlin, Germany*

(Received 22 November 2013; revised manuscript received 9 January 2014; published 29 January 2014)

The low temperature ($T = 5$–40 K) capture of free electrons into hydrogenlike antimony centers in germanium has been studied by a time-resolving experiment using the free electron laser FELBE. The analysis of the pump-probe signal reveals a typical capture time of about 1.7 ns that decreases with pump energy to less than 1 ns while the number of ionized donors increases. The dependence on the pump-pulse energy is well described by an acoustic phonon-assisted capture process. In the cases when (i) a significant number of the electrons is in the conduction band (flux densities larger than 5×10^{25} photons/(cm^2 s), (ii) the lattice temperature is above $\sim$20 K, or (iii) a static electric field above $\sim$2 V/cm is applied to the crystal, the pump-probe technique reveals an additional intraband relaxation process with a characteristic time of $\sim$100 ps, which is much shorter than that of the capture of free electrons into the antimony ground state.

DOI: 10.1103/PhysRevB.89.035205 PACS number(s): 78.47.db, 81.05.Cy, 71.55.−i

I. INTRODUCTION

Impurity centers in semiconductors such as silicon (Si) or germanium (Ge) have been thoroughly investigated over the last decades. Most of the research in the early years was devoted to the low temperature equilibrium spectroscopy of impurity states, measurements of photocurrent relaxation, and the study of recombination process when carriers are captured by ionized centers [1–4].

Time-resolved spectroscopy of excited bound impurity states in semiconductors has attracted significant interest in recent years. This has been triggered by potential benefits of impurity states in quantum computing for realizing lasers or as model systems for astronomic research [5–11]. For hydrogenlike centers in Si, such time-resolved studies have been performed using a pump-probe technique and a picosecond-pulsed free electron laser (FEL). Typical relaxation times range from a few 10 ps up to $\sim$200 ps for intracenter excitation, i.e., photoexcitation from the ground state into one of the excited states [12–15].

Impurity centers in Ge are the basis for terahertz (THz) lasers and broadband THz detectors [16–18]. Shallow impurities in Ge, such as antimony (Sb) and gallium (Ga), allow for the detection of radiation down to about 2.5 THz and by applying uniaxial stress down to $\sim$1.5 THz in Ge:Ga [16]. Such detectors were used on several space-borne astronomical observatories such as the Herschel Space Observatory [19], the Spitzer Space Telescope [20], and the Akari satellite [21]. Recently, these detectors were installed in the Field-Imaging Far-Infrared Line Spectrometer (FIFI-LS) on the Stratospheric Observatory for Infrared Astronomy (SOFIA) [22]. Understanding of the relaxation dynamics of free carriers in Ge will help to improve the performance of extrinsic Ge photoconductors.

Relaxation dynamics in undoped bulk and nanowire Ge using optical-pump with optical-probe [23] or terahertz-probe [24] spectroscopy have revealed important information about electron-hole recombination. However, relaxation dynamics of ionized centers in Ge were investigated with a considerable number of different but mainly indirect methods. These include studies of the electric field-dependent stationary photoconductive signals induced by short THz pulses [1], temperature-dependent intensities of photothermal ionization lines with modulated submillimeter sources [2,3], or optical saturation of the photoconductive response as well as the absorption coefficient [25–27]. Other indirect methods looked at the temperature dependence of the hole mobility [28] or the detection bandwidth [29] as well as the generation-recombination noise [30] in heterodyne detection systems. The shortest recombination times of ionized and excited carriers, which were calculated, ranged from a few hundred picoseconds [1,27] to several microseconds [26] depending strongly on the doping concentration as well as on the compensation level. To overcome the problems stemming from uncertainties in different parameters needed to calculate recombination times, direct measurements are preferable.

A direct measurement of short pulses from a THz FEL with a neutron transmutation-doped *p*-Ge detector and a fast readout circuit yielded a recombination time of about 2 ns [31]. The analysis of relaxation of the photoconductivity after short voltage pulses [32] and optical THz pulses [33] resulted in time constants of about 10 ns in both cases. Contactless direct pump-probe measurements presenting intervalence band relaxation dynamics of Ga in highly doped ($N_A \sim 10^{16}$–10^{17} cm^{-3}) Ge were carried out at wavelengths between 4 and 12 μm [34,35].

A fundamental temporal analysis in the THz region of moderately doped Ge using a direct method devoid of additional effects such as an electric field has not been conducted

until now. We present an analysis of the relaxation of free electrons in Ge doped with Sb (Ge:Sb) which are photoionized in the state continuum close to the conduction band (CB) edge. The measurements were carried out with a dedicated pump-probe experimental setup at the free electron laser FELBE of the Helmholtz-Zentrum Dresden-Rossendorf. The analysis of dependences of capture times on the photoexciting laser intensity helps to understand the underlying relaxation processes. It also gives the fundamental temporal limit of this material system when used as THz photodetectors.

II. ELECTRONIC CAPTURE BY HYDROGENLIKE CENTERS IN SEMICONDUCTORS

Theoretical work on the recombination kinetics of shallow impurities dates back to the 1960s when M. Lax [36] introduced the cascade capture model. This was later refined by different authors, in particular by Abakumov, Perel', and Yassievich (APY) [37] and by Ascarelli and Rodriguez [38]. The cascade model assumes that the main capture process is a multistep relaxation accompanied by the emission of acoustic phonons. Since our study focuses on n-type Sb-doped Ge, we will first discuss the relaxation processes in this material with respect to the cascade model and its refinements. The energy levels of the Sb donor can be described in the frame of the effective mass theory (EMT). Deviations from the EMT occur in particular for s-type states that have significant amplitudes close to the donor ion. This causes a splitting of the states, the so-called chemical splitting. It is most pronounced for the $1s$ ground state, which splits into a $1s(A_1)$ singlet and a $1s(T_2)$ triplet (Fig. 1). A free electron in Ge:Sb first relaxes to the CB minimum, losing its energy by emission of acoustic phonons. The electron turns out to be captured by one of the Sb excited states only when its binding energy exceeds kT_e (T_e is the temperature of the electron gas). The electron

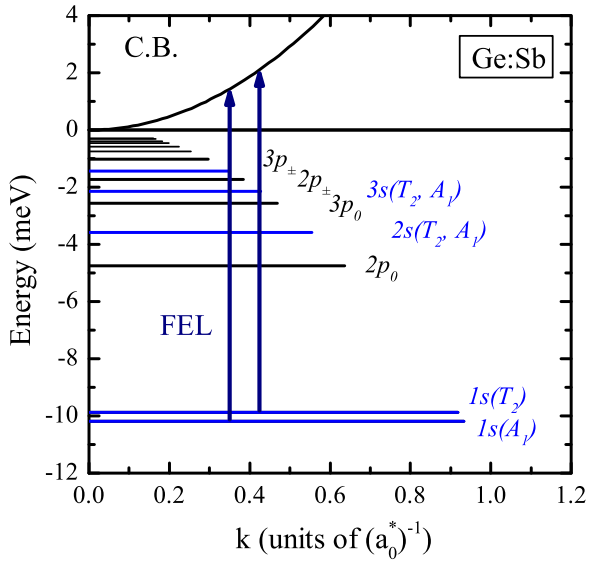

FIG. 1. (Color online) Discrete energy levels of Sb impurity in germanium bound to the minimum of the conduction band (CB) [4]. Only the $1s(A_1)$ and $1s(T_2)$ states are significantly populated at 4.5 K. The arrows indicate the photoionization by the FEL at a wavelength of 105 μm.

relaxes further through a cascade of bound states emitting acoustic phonons (phonon-assisted process). Finally it ends in the impurity $1s(A_1)$ and $1s(T_2)$ ground states. It is worth noting that transitions between even-parity s-type states have larger relaxation rates, and that they dominate the process [38].

However, there exists an energy region near the CB edge $E = 0$ meV in which the interference of different ionized centers on the capture process become important, and it is necessary to take into account the large-scale fluctuation of the potential E_0 of such centers [37]. Here $E_0 \approx e^2\varepsilon^{-1}N_+^{1/3}$, where e is the electron charge, ε is the dielectric constant, and N_+ is the number of ionized donors. If $kT > E_0$, the electrons become thermalized ($T = T_e$), the single center approach is valid, and the capture rate $\nu_+ = N_+\sigma v$, where σ is the recombination cross section of a single center and v is the electron velocity. This case implies small densities of ionized centers and the capture time constant $\tau_+ = \nu_+^{-1}$ is inversely proportional to their number. According to APY the presence of many centers cannot be ignored when $N_+ > N_{\text{crit}} = (kT\varepsilon e^{-2})^3$ or $kT < E_0$, and the relaxation time as shown [37] is given by

$$\tau_+ \approx \frac{\pi\hbar^4\rho}{2m^{5/2}E_D^2}\sqrt{\frac{1}{2E_0}} = \frac{\pi\hbar^4\rho\sqrt{\varepsilon}}{2m^{5/2}eE_D^2}N_+^{-1/6}, \qquad (1)$$

where E_D is the constant of the deformation potential, m is the carrier effective mass, and ρ is the density of the crystal. For further calculations, E_D is approximated by the shear deformation potential constant of the CB of Ge ($\Xi_u = 16.4$ eV) [39]. Equation (1) implies that the photoexcited carriers are captured on the state of the fluctuation potential with the time being weakly dependent on the number of ionized centers, $\tau_+ \sim N_+^{-1/6}$. This estimate apparently gives a shorter time of capture into the ground state, measured in a pump-probe experiment, because the intracenter relaxation from binding energies lower kT is not included in the theory.

Recombination times can be directly measured in the time domain using a pump-probe technique. This requires the irradiation of the sample with a short optical pulse, i.e., the pulse duration is much shorter than the characteristic times of the involved decay processes. In the case of Ge:Sb, the typical FEL pulses are in the order of a few picoseconds, which is shorter than the expected electronic decay times. Under the intense illumination (high excitation) by an FEL, the conditions for applying a single center model are typically not met. At $T = 5$ K, the critical value is $N_{\text{crit}} \approx 10^{14}$ cm^{-3}. As we will see later, this accounts for about 10% of the impurity concentration in our Ge:Sb samples. It is important to note that additional capture centers always exist in unexcited semiconductors due to residual impurity compensation. Therefore the high excitation regime occurs at an even smaller number of ionized centers. As already noted, the dependence of the recombination time on the number of optically ionized centers in the low excitation regime ($N_+ < N_{\text{crit}}$) is $\tau_+ \sim N_+^{-1}$. In the high excitation regime ($N_+ > N_{\text{crit}}$), this dependence is $\tau_+ \sim N_+^{-1/6}$. In the case of a pump-probe measurement, one has to consider the high excitation case and in the simplest case a rate equation approach with a two-level system according to

$$\frac{dN_+}{dt} = -\frac{1}{\tau_+}N_+\Big|_{N_+ \gg N_{\text{crit}}}, \quad \frac{1}{\tau_+} : N_+^{\frac{1}{6}}. \qquad (2)$$

Equation (2) can be solved analytically to $N_+(t) = 1/(N_+(0)^{-1/6} + pt)^6$, where $p = 1/\tau_+ N_+(0)$. However, because of the weak dependence of the relaxation time on the density of recombination centers, this function can be approximated with a single exponential decay. The time constant of this exponential is a function of the initial concentration of the ionized centers $N_+(0)$ and the number of ionized centers as a function of time is given by

$$N_+(t) \cong N_+(0) \cdot e^{-\frac{t}{\tau_+(N_+(0))}}. \quad (3)$$

It should be noted that in the low-excitation regime the two-level rate-equation model yields a rational function of the type $N_+(t) = N_+(0)/(1 + pt)$, where p is a fitting parameter.

The situation becomes more complicated when the majority of carriers are in the CB. That can be achieved at high pump power and external field excitation of a bound electron. In this case intraband absorption will play a significant role. Also when the temperature of the Ge crystal is increased, thermal excitation of the electrons leads to an increase of the popoulation of the excited states and in the CB. At 5 K the population of the excited states and the CB is negligible. However, above ~10 K it cannot be neglected anymore, and when the temperature reaches 30 K almost all electrons are in the CB. When an electric field is applied to the crystal, two effects have to be considered. The first is the direct influence of the electric field on the recombination time, and the second is the heating of the Ge lattice due to ohmic losses in the crystal. The latter effect occurs when the current becomes large. Above a certain field, typically ~2 V/cm, all electrons are in the CB. In all of these cases, the pump-probe technique does not only measure the recombination time from the CB to the ground state, but it also measures the intraband relaxation because electrons in the CB are excited by the pump pulse and the probe pulse detects the change of transmission induced by the pump pulse. This intraband absorption and its characteristic time is described by another exponential decay similar to Eq. (3).

III. EXPERIMENTAL SETUP AND SAMPLE PREPARATION

The capture rate of free charge carriers can be experimentally determined by measuring the decay of a nonequilibrium population of free cariers. One of the direct procedures is the so-called optical pump-probe technique. It measures the photoinduced changes of the transmittance of a sample caused by the formation of a nonequilibrium carrier population. Advantages of the pump-probe technique are the absence of any significant perturbation of the investigated system, such as, for example, an external electric field, the high temporal resolution achieved by the application of short-pulsed lasers, and the possibility for resonant excitation provided by frequency-tunable FELs. Assuming an instantaneous excitation by the pump pulse, which is approximately constant through the probed sample with a thickness d, an absorption coefficient $\alpha(t)$, and a single-path in the probed sample, the probe transmission can be written as [40]: $T(t) \approx (1 - R)^2 \exp[-\alpha(t)d]$, where R is the reflection coefficient at the surface of the sample. Provided the probe transmission without pump pulse $T_0(t)$ is known, one gets a pump-probe signal $\Delta T/T$, which is independent on reflection and absorption:

$$\frac{\Delta T(t)}{T(t)} = \frac{T(t) - T_0(t)}{T_0(t)} \approx e^{-\Delta\alpha(t)d} - 1 = e^{-\sigma\Delta N(t)d} - 1. \quad (4)$$

Here $\Delta\alpha(t) = \sigma\Delta N(t)$ is the pump-induced change of the absorption coefficient, σ is the absorption cross section, and $\Delta N(t) = N(t) - N_0(t)$ is the pump-induced change of the concentration of excited carriers. The latter is equal to the difference between the populations of the probed states, i.e., ground Sb states relative to the CB (bottom of Fig. 1). Usually special attention is paid in the pump-probe experiment to ensure that the absorption of the sample is small, i.e., $\sigma N(t)d \ll 1$. In this case the measured pump-probe signal is directly proportional to the population difference, $\Delta T/T \approx \sigma\Delta N(t)d$.

The sample was a Czochralski-grown Ge:Sb crystal with dimensions of $10 \times 10 \times 0.5$ mm^3. The 10×10 mm^2 surfaces that face the pump and probe beams were wedged. The Sb impurity concentration N_D was chosen to be $\sim 1 \times 10^{15}$ cm^{-3}, and the residual compensation was estimated to be <0.1%. This guaranteed high enough absorption when an impurity-band formation has not yet formed. Furthermore, the APY predicts short recombination times in the nanosecond range for $N_D > 10^{13}$ cm^{-3} at high photon fluxes. The low-temperature absorption spectrum of the sample (Fig. 2) was measured with a Fourier-transform infrared spectrometer and confirmed that Sb centers are the dominant species. Furthermore, it was confirmed that the low absorption approximation ($\sigma N(t)d \ll 1$) holds for the pump energy of 11.8 meV (wavelength 105 μm).

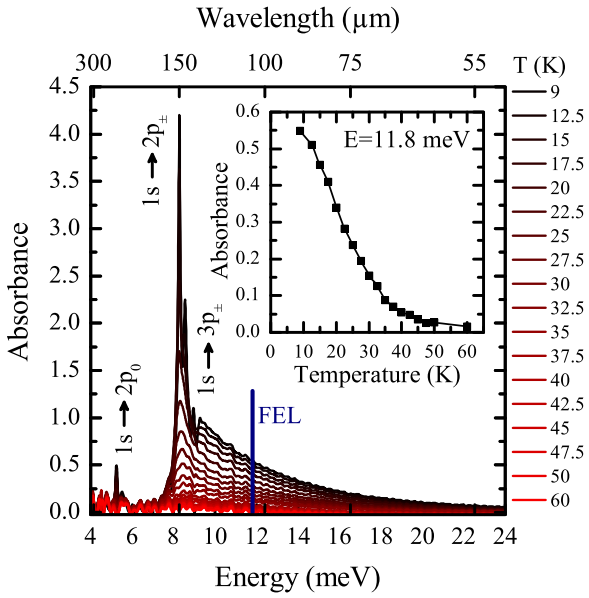

FIG. 2. (Color online) Absorbance (σNd) of the investigated Ge:Sb sample as a function of the temperature, showing spectral features corresponding to intracenter (discrete lines) and impurity-band transitions (continuum at energies larger than ~10 meV). The discrete lines correspond to transitions originating from the $1s(A_1)$ and $1s(T_2)$ antimony states, which is thermally populated. Inset: Absorbance in the sample at the FEL pump photon energy of 11.8 meV (105 μm) as a function of the sample temperature.

The sample was mounted in a liquid-He (l-He) flow cryostat equipped with diamond windows and cooled to approximately 5 K. By changing the flow of l-He through the cryostat, the temperature of the sample was varied between 5 K and 40 K. The temperature was measured with a sensor mounted on the sample holder in vicinity to the sample.

FELBE provides pulses at a repetition rate of 13 MHz. At the wavelength of our experiments (105 μm), the pulses are Gaussian shaped with a full width at half-maximum (FWHM) of $\approx$10 ps. For the pump-probe experiments, we used the same optical layout as in Ref. [41]; each FEL pulse was split by a Mylar beam splitter into a pump and a probe pulse. The pump pulse contained about 95% of the total energy, and the rest was in the probe pulse. Both pulses were focused to a spot of ~400-μm diameter on the Ge:Sb sample. The probe pulse impinges on the sample at a slight angle with respect to each other and almost normal incidence with respect to the surface of the sample. The pump radiation that passed the sample was blocked by an absorber. The polarization of the probe pulse was rotated by 90° with respect to the pump pulse, and an additional polarizer was set in front of the detector in order to minimize contributions from scattered pump radiation. The time delay of the probe pulse with respect to the pump pulse was provided by an optical delay stage. The temporal range for this delay is limited on one side by the duration of the pump and probe pulses and on the other side by the longest optical path difference (~50 cm) between pump and probe pulses. In our experiments, this range was between ~10 ps and 1.6 ns. The pump beam was mechanically chopped at 350 Hz, and the probe signal was detected with a silicon bolometer and a lock-in amplifier that uses the chopper frequency as reference. In Eq. (4), the signal ΔT is the transmission of a probe when pump modulation is on (chopper blade opened) relative to the transmission when the pump beam is off (chopper blade closed). To obtain the relative change, $\Delta T/T$, the reference signal, T, of the setup was measured by mechanically chopping the probe beam.

The average FEL power was measured with a pyroelectric power meter. The maximum average power was 72 mW, corresponding to about 5.5 nJ pulse energy or a photon flux density of 1×10^{26} cm^{-2} s^{-1}, taking into account the reflections from the window and the sample's surface, respectively. It could be reduced with two diffractive attenuators in steps of 3 dB, 5 dB, and 10 dB. One was used to attenuate the total pulse, and the other was used to attenuate the pump pulse only. The wavelength of the FEL was chosen in such a way that it corresponds on one hand to the excitation energy for a transition from the $1s(A_1)$ and $1s(T_2)$ states into the bottom of the CB (blue arrows in Fig. 1); however, on the other hand, the atmospheric absorption has to be small. At this wavelength, the FEL pulse duration is bandwidth limited with a FWHM of 10 ps.

IV. RESULTS AND DISCUSSION

In Fig. 3 the pump-probe signal is shown for a number of different pump-pulse energies. In general the smaller the pump energy the smaller is the pump-probe signal. This is shown in the inset of Fig. 3 where the pump-probe signal at zero delay is plotted against the pump-pulse energy. In our experiments, the pump-probe signal has always the same sign,

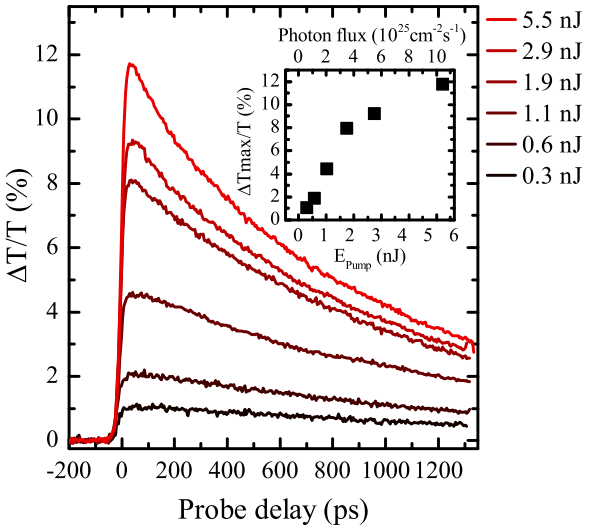

FIG. 3. (Color online) Pump-probe signals of the Ge:Sb sample for different pump-pulse energies. Inset: Dependence of the maximum of the relative transmission on the pump pulse energy at 105 μm excitation wavelength. The temperature of the Ge:Sb sample was ~5 K.

which corresponds to a pump-induced change of transmittance between 1% and 12%. Up to pump-pulse energies of ~2 nJ, the change of transmittance $\Delta T/T$ increases linearly. Above that value it tends to saturate. This indicates a change in total absorption due to increased free-carrier absorption.

In order to estimate conditions for high-excitation regime, we calculate the number of ionized centers for the lowest pump-pulse energy used in the experiment, 0.3 nJ. This pulse energy, reduced by reflections from the diamond window and the sample itself, corresponds to the photon flux on the sample surface of about $\Phi \approx 4.8 \times 10^{24}$ cm^{-2} s^{-1}. The ionization cross section is $\sigma \approx 1.6 \times 10^{-14}$ cm^2 [4]. Then a lower limit of photoionized coulomb centers $N_+/N_D = \tau_+ \times \Phi \times \sigma$ (and, correspondingly, photoionized electrons, N) of 10%, which, according to the APY theory, would result in the decay time law proportional to $N_+^{-1/6}$, would be reached for free-electron capture time $\tau_+ > 1.3$ ps, which is much shorter than excitation-pulse duration. This justifies the assumption of fitting with an exponential function [Eq. (2)]. Since pump and probe pulses have non-negligible duration, which is larger than the temporal resolution of the delay line, we assigned a Gaussian profile to the pulses and took this into account in the fitting procedure. This leads to the following fit function, $S(t)$, which is a convolution of the Gaussian pulse with the dynamic population $N_+(t)$ [Eq. (2)]:

$$S(t) = a \cdot e^{\frac{(t-t_0)^2}{2\Delta t^2}} * e^{-\frac{t}{\tau_+}}. \quad (5)$$

Here Δt is the width of the probe pulse, and t_0 is the time of maximum overlap between pump and probe pulses, a is a fit parameter, and τ is the time constant for the high excitation case. The use of the estimated pulse duration Δt of 10 ps as a fixed parameter led to excellent fitting results (Figs. 4 and 5). As a confirmation, we included the pulse duration in the fitting procedure and consistently obtained values ω of 9.5 ± 1 ps. At pump energies up to ~5.5 nJ, the maximum of the pump-probe

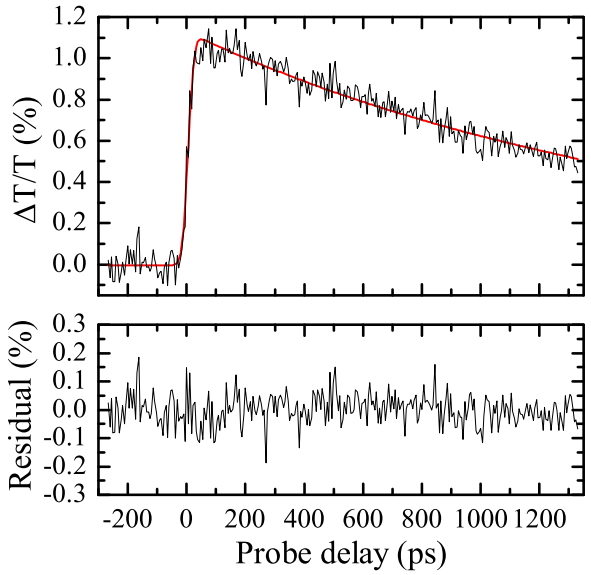

FIG. 4. (Color online) Pump-probe signal of the Ge:Sb sample at a pump-pulse energy of 0.3 nJ and a temperature of ~5 K. The straight red line is a fit using Eq. (6). The decay time is 1.7 ns. The residual is the difference between fit and measurement.

signal increases linearly (inset of Fig. 3). In this case the single exponential function fits the measured results very well. An example for a fit with low pump energy is shown in Fig. 4. The residual is the difference between fit and measurement. As can be seen, the fit resembles the pump-probe signal very well. The decay time in this case is 1.7 ± 0.1 ns. Given the simplifications of the APY, this result agrees very well with the

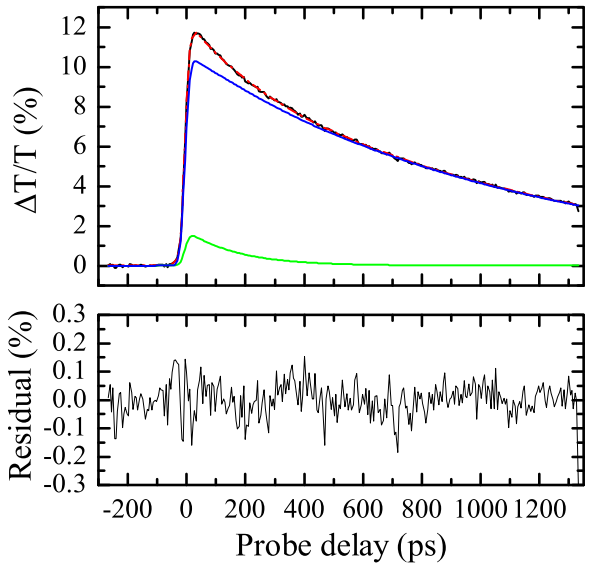

FIG. 5. (Color online) Pump-probe signal of the Ge:Sb sample at a pump-pulse energy of 5.5 nJ. In this case the fit parameter b is about 20% of a, which indicates that intraband processes are significant. The straight blue line is the calculated contribution to the total signal caused by phonon-mediated capture using the fit parameters a and τ_+. The straight green line is the same but for intraband processes using the fit parameters b and τ_i. The residual is the difference between fit and measurement.

theoretical value of $\tau_+ \approx 0.6$ ns, calculated using Eq. (1) for $N_+ = N_{\text{crit}}$ and $T = 5$ K. As explained above, the theoretical recombination time is smaller than the value determined by our experiment. This is due to the fact that, in contrast to the experimental recombination time, the APY does not include the excited donor relaxation time down to the ground state. In order to confirm that the experiments were performed in the high-excitation regime, we have fitted a convolution of a Gaussian pulse with rational function to the pump-probe signals. As described in Sec. II, this approach is applicable in the low-excitation regime. However, the fitting procedure did not yield a result of similar quality as the fit in Eq. (3).

With increasing pump power (at 3 nJ and 5.5 nJ) the pump-probe signal cannot be fitted with a single exponential function anymore. Another exponential decay with a characteristic time τ_i has to be added to Eq. (5):

$$S(t) = \mathrm{e}^{\frac{(t-t_0)^2}{2\Delta t^2}} * (a \cdot e^{-\frac{t}{\tau_+}} + b \cdot e^{-\frac{t}{\tau_i}}). \tag{6}$$

Figure 5 shows the fit result and both exponential contributions separately. The magnitude of the second exponential function, i.e., the fit parameter b in Eq. (6), reaches about 20% of parameter a at the highest pump-pulse energy of 5.5 nJ. The decay time τ_i is 100 ± 50 ps. When fitting Eq. (6) to the pump-probe signals at lower pump energies, the parameter b converges to 0. This indicates that the second exponential term describes another process with a characteristic time of ~100 ps. At large fluxes, the occupation of the CB is of the same order of magnitude or even larger than that of the ground state. An estimation [42] of the intraband absorption by free electrons gives a much smaller absorption cross section of 1.5×10^{-16} cm^2 compared to 1.6×10^{-14} cm^2 for impurity ionization and can only be observed for large photon fluxes. As estimated above, the time for the impurity ionization process is in the order of magnitude of the FEL pulse width. Thus, contribution of intraband excitation of free carriers can occur within the duration of the FEL pulse. And carriers with an excess energy of ~10 meV are generated in the CB. The intraband relaxation rate due to interaction of these electrons with long-wave acoustical phonons can be estimated by APY [Eq. (1)]. Substituting E_0 with the additional energy of about 10 meV yields a relaxation time of about 120 ps and fits well to the decay of the second relaxation component in the pump-probe signal [Eq. (6)].

In Fig. 6, the capture time τ_+ is plotted as a function of the pump-pulse energy. The dashed line is the theoretically predicted dependence of the capture time on the pump-pulse energy. Since the number of ionized donors is proportional to the pump-pulse energy E_{Pump}, the APY theory predicts $\tau_+ \sim E_{\text{Pump}}^{-1/6}$. Within the measurement uncertainty, the APY theory describes the experiment very well, and the measurements confirm the acoustic-phonon mediated capture by ionized donors. Similar time constants for n-Ge have been shown in previous work. Saturation experiments at 10.6 μm [25] and 90 μm [27] with n-Ge resulted in modeled time constants from 680 ps up to 1 ns, respectively. These were interpreted with the $2s \rightarrow 1s$ transition in accordance with the recombination model by Ascarelli and Rodriguez [38]. The main drawback of these experiments is the necessity of a wide range of photon flux densities necessary to obtain a single time constant, which

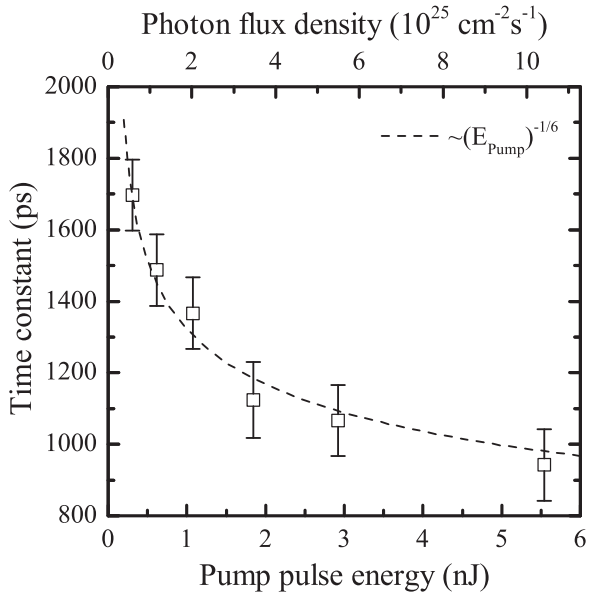

FIG. 6. Time constant τ_+ as a function of the pump-pulse energy. The dashed curve is a fit according to the APY theory [37].

is, as shown here, a function of the photon flux density itself. Another indirect approach by measuring the bandwidth as well as the amplitude of the generation-recombination noise of a heterodyne system at 118 μm employing a set of n-Ge samples with $N_D \sim (1-2) \times 10^{15}$ cm^{-3} and a compensation of 10–50% revealed recombination times as low as 1.1 ns [29,30]. In this case the influence of the sample geometry and of the electronic circuitry may have distorted the results, and focus was laid mostly on practical aspects of the heterodyne systems. One of the key issues, i.e., the influence of the recombination centers by varying the photon flux density, was not addressed as well.

V. INFLUENCE OF TEMPERATURE AND ELECTRIC FIELD

In Fig. 7, the time constants of the pump-probe signal are shown as a function of the temperature of the Ge:Sb sample for a pump-pulse energy of 2 nJ. The fitting procedure was the same as described in the previous section for the high pump-power results, i.e., two exponentials convoluted with a Gaussian pulse of 10 ps FWHM were fitted to the pump-probe signal. Each of the time constants, τ_+ and τ_i, belongs to one of the exponential functions. At 15 K and below, as well as at 40 K, one exponential function was sufficient to fit the pump-probe signal. Only at 20 K and 30 K both exponential functions were necessary to obtain a good fit. Since below 15 K only few carriers are in the CB either through thermal excitation or by excitation with the pump pulse, the recombination process is dominated by a cascade acoustic-phonon mediated capture, and the corresponding characteristic time is approximately 1.2 ns, as described in the previous section. At 20 K and at 30 K, two processes prevail: capture with a characteristic time of 1.3 ± 0.5 ns and intraband relaxation with a characteristic time of 100 ± 50 ps. At 40 K, essentially all electrons are thermally excited into the CB, and

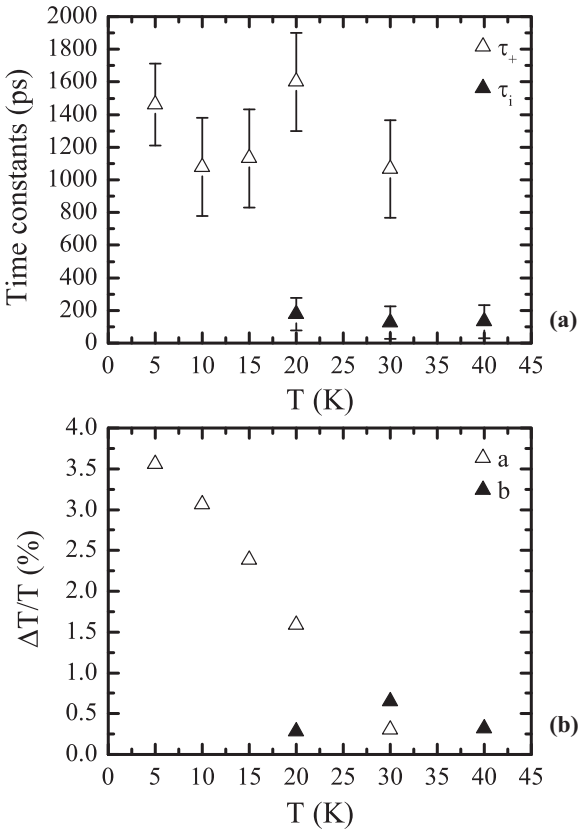

FIG. 7. (a) Time constants τ_+ and τ_i for a biexponential fit as a function of the heat sink temperature. For temperatures lower than 20 K, a single exponential was used. At 20 K and above, a second exponential [Eq. (6)] has to be included in order to obtain a good fit of the measured data. (b) Amplitude fit parameters a, b of the biexponential fit [Eq. (6)].

the only process that can be measured with the pump-probe technique is the intraband relaxation. It is worth noting that within the accuracy of the measurements, the time constants for both processes, acoustic-phonon mediated capture and intraband relaxation, are independent of the temperature.

Finally, we have measured the influence of an electric field on the relaxation process (Fig. 8). In order to do so, ohmic contacts were manufactured to opposing edges of the Ge:Sb crystal. The distance between the contacts is 10 mm. The voltage was supplied by a Keithley 2430 source meter. The fitting procedure is the same as for the temperature measurements, i.e., Eq. (6) was fitted to the pump-probe signal. Again two time constants are extracted: 1.6 ± 0.5 ns and 200 ± 50 ps. Below 2 V/cm, only the process with a long time constant exists, and at 6 V/cm and above only the process with the short time constant exists. For intermediate fields both processes prevail, but the magnitude of the short process increases with increasing electric field, as deduced from the relative strength of the fitting parameters a and b. Within the uncertainty of the measurement and fitting procedure, both time constants are independent of the electric field. The process with the long time constant is the acoustic-phonon mediated capture of electrons by the Sb donor centers. The process with the short time constant is due to intraband scattering. At an

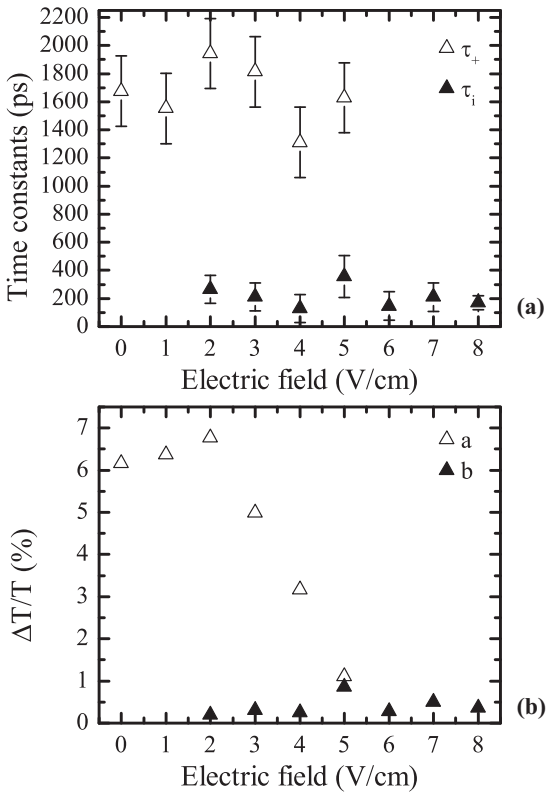

FIG. 8. (a) Time constants τ_+ and τ_i for a biexponential fit as a function of the electric field. At electric fields higher than ∼2 V/cm, the second exponential decay [Eq. (6)] has to be included in order to fit the measured data. (b) Amplitude fit parameters a, b of the biexponential fit [cf. Eq. (6)].

electric field of ∼2 V/cm, electrical breakdown occurs in the sample, and the resistance drops from a few kΩ to 300 Ω. The electrically dissipated power is less than 200 mW. Therefore, heating of the sample by the current can be neglected. In fact, the temperature measured by the sensor did not increase. At fields above 2 V/cm, donor electrons are electrically excited into the CB. The electrons are further excited by the pump pulse, and the probe pulse measures their relaxation. At the highest field, basically all electrons are in the CB, and recombination with the ionized Sb donors is negligible. It is worth noting that the intraband process has about the same time constant independent whether it is caused by high pump energy, high temperature, or a large static electric field.

VI. SUMMARY AND CONCLUSION

We have conducted a study of the electron relaxation processes in photoexcited n-type Ge:Sb at temperatures from 5 to 40 K. A dedicated single-color pump-probe experiment based on an FEL enabled the determination of the intraband relaxation time (∼100 ps) and the capture time of photoexcited electrons. The time constant of this capture process decreases from 1.7 ns to 1 ns with increasing pump power because the number of ionized Sb donors increases. This decrease is proportional to $E_{\mathrm{Pump}}^{-1/6}$, as predicted by the APY theory [37]. At a temperature of 5 K, the phonon-mediated capture process dominates. However, when the temperature is increased or when an electric field is applied, the relative strength of both processes changes and eventually vanishes above 30 K or 5 V/cm. Finally it should be noted that due to the short time constants, Ge:Sb is well suited as material for fast THz detectors.

ACKNOWLEDGMENTS

This work was funded by the German Federal Ministry of Education and Research Grant No. 05K10KTD and by the Scientific Program of the Russian Academy of Sciences, Program No. 24. N.D. acknowledges support by the Helmholtz Research School on Security Technologies.

[1] F. Kohl, W. Müller, and E. Gornik, Infrared Phys. **18**, 697 (1978).
[2] E. M. Gershenzon, G. N. Gol'tsman, and N. G. Ptitsina, Zh. Eksp. Teor. Fiz. **76**, 711 (1979) [Sov. Phys. JETP **49**, 355 (1979)].
[3] E. M. Gershenzon, G. N. Gol'tsman, V. V. Multanovskii, and N. G. Ptitsina, Zh. Eksp. Teor. Fiz. **77**, 1450 (1979) [Sov. Phys. JETP **50**, 728 (1979)].
[4] A. K. Ramdas and S. Rodriguez, Reports Prog. Phys. **44**, 1297 (1981).
[5] B. E. Kane, Nature **393**, 133 (1998).
[6] S. G. Pavlov, R. K. Zhukavin, E. E. Orlova, V. N. Shastin, A. V. Kirsanov, H.-W. Hübers, K. Auen, and H. Riemann, Phys. Rev. Lett. **84**, 5220 (2000).
[7] H.-W. Hübers, S. G. Pavlov, and V. N. Shastin, Semicond. Sci. Technol. **20**, S211 (2005).
[8] H. Haffner, C. F. Roos, and R. Blatt, Phys. Rep. **469**, 155 (2008).
[9] P. T. Greenland, S. Lynch, A. F. G. van der Meer, B. N. Murdin, C. R. Pidgeon, B. Redlich, N. Q. Vinh, and G. Aeppli, Nature **465**, 1057 (2010).
[10] B. N. Murdin, J. Li, M. L. Y. Pang, E. T. Bowyer, K. L. Litvinenko, S. K. K. Clowes, H. Engelkamp, C. R. Pidgeon, I. Galbraith, N. V. Abrosimov, H. Riemann, S. G. Pavlov, H.-W. Hübers, and P. G. Murdin, Nat. Commun. **4**, 1469 (2013).
[11] S. G. Pavlov, R. K. Zhukavin, V. N. Shastin, and H.-W. Hübers, Phys. Status Solidi **250**, 9 (2013).
[12] N. Q. Vinh, P. T. Greenland, K. L. Litvinenko, B. Redlich, A. F. G. van der Meer, S. Lynch, M. Warner, A. M. Stoneham, G. Aeppli, D. Paul *et al.*, Proc. Natl. Acad. Sci. **105**, 10649 (2008).
[13] S. A. Lynch, G. Matmon, S. G. Pavlov, K. L. Litvinenko, B. Redlich, A. F. G. van der Meer, N. V. Abrosimov, and H.-W. Hübers, Phys. Rev. B **82**, 245206 (2010).
[14] H.-W. Hübers, S. G. Pavlov, S. A. Lynch, Th. Greenland, K. L. Litvinenko, B. Murdin, B. Redlich, A. F. G. van der Meer, H. Riemann, N. V. Abrosimov, P. Becker, H.-J. Pohl, R. Kz. Zhukavin, and V. N. Shastin, Phys. Rev. B **88**, 035201 (2013).
[15] N. Q. Vinh, B. Redlich, A. F. G. van der Meer, C. R. Pidgeon, P. T. Greenland, S. A. Lynch, G. Aeppli, and B. N. Murdin, Phys. Rev. X **3**, 011019 (2013).
[16] E. E. Haller, Infrared Phys. Technol. **35**, 127 (1994).

[17] E. Bründermann, in *Long-Wavelength Infrared Semiconductor Lasers*, edited by H. K. Choi (John Wiley & Sons, Inc., New York, 2005), pp. 279–350.
[18] J. Farhoomand, D. Sisson, and J. W. Beeman, Infrared Phys. Technol. **51**, 102 (2007).
[19] A. Poglitsch, C. Waelkens, N. Geis, H. Feuchtgruber, B. Vandenbussche, L. Rodriguez, O. Krause, E. Renotte, C. van Hoof, P. Saraceno, J. Cepa, F. Kerschbaum, P. Agnèse, B. Ali, B. Altieri, P. Andreani, J.-L. Augueres, Z. Balog, L. Barl, O. H. Bauer *et al*., Astron. Astrophys. **518**, L2 (2010).
[20] G. H. Rieke, E. T. Young, C. W. Engelbracht, D. M. Kelly, F. J. Low, E. E. Haller, J. W. Beeman, K. D. Gordon, J. A. Stansberry, K. A. Misselt, J. Cadien, J. E. Morrison, G. Rivlis, W. B. Latter, A. Noriega-Crespo, D. L. Padgett, K. R. Stapelfeldt, D. C. Hines, E. Egami, J. Muzerolle *et al*., Astrophys. J. Suppl. Ser. **154**, 25 (2004).
[21] M. Fujiwara, T. Hirao, M. Kawada, H. Shibai, S. Matsuura, H. Kaneda, M. Patrashin, and T. Nakagawa, Appl. Opt. **42**, 2166 (2003).
[22] S. Colditz, F. Fumi, N. Geis, R. Hönle, R. Klein, A. Krabbe, L. Looney, A. Poglitsch, W. Raab, M. Savage, F. Rebell, and C. Fischer, Proc. SPIE **8446**, 844611 (2012).
[23] R. P. Prasankumar, S. Choi, S. A. Trugman, S. T. Picraux, and A. J. Taylor, Nano Lett. **8**, 1619 (2008).
[24] J. H. Strait, P. A. George, M. Levendorf, M. Blood-Forsythe, F. Rana, and J. Park, Nano Lett. **9**, 2967 (2009).
[25] J. B. McManus, R. People, R. L. Aggarwal, and P. A. Wolff, J. Appl. Phys. **52**, 4748 (1981).
[26] G. Jungwirt and W. Prettl, Infrared Phys. **32**, 191 (1991).
[27] T. Theiler, H. Navarro, R. Till, and F. Keilmann, Appl. Phys. A **56**, 22 (1993).
[28] O. D. Dubon, Jr., I. Wilke, J. W. Beeman, and E. E. Haller, Phys. Rev. B **51**, 7349 (1995).
[29] G. Dodel, J. Heppner, E. Holzhauer, and E. Gornik, J. Appl. Phys. **54**, 4254 (1983).
[30] I. S. Park, E. E. Haller, E. N. Grossman, and D. M. Watson, Appl. Opt. **27**, 4143 (1988).
[31] F. A. Hegmann, J. Williams, B. Cole, M. Sherwin, J. W. Beeman, and E. E. Haller, Appl. Phys. Lett. **76**, 262 (2000).
[32] M. S. Kagan, I. V. Altukhov, V. P. Sinis, and S. K. Paprotskiy, J. Phys. Conf. Ser. **193**, 012034 (2009).
[33] S. V. Morozov, K. V. Marem'yanin, I. V. Erofeeva, A. N. Yablonskiy, A. V. Antonov, L. V. Gavrilenko, V. V. Rumyantsev, and V. I. Gavrilenko, Semiconductors **44**, 1476 (2010).
[34] M. Woerner, T. Elsaesser, and W. Kaiser, Phys. Rev. B **45**, 8378 (1992).
[35] M. Woerner, W. Frey, M. T. Portella, C. Ludwig, T. Elsaesser, and W. Kaiser, Phys. Rev. B **49**, 17007 (1994).
[36] M. Lax, Phys. Rev. **119**, 1502 (1960).
[37] V. N. Abakumov, V. I. Perel', and I. N. Yassievich, Zh. Eksp. Teor. Fiz. **72**, 674 (1977) [Sov. Phys. JETP **45**, 354 (1977)].
[38] G. Ascarelli and S. Rodriguez, J. Phys. Chem. Solids **22**, 57 (1961).
[39] P. Baranskii and V. Kolomoets, Phys. Status Solidi **5**, K1 (1971).
[40] P. C. Findlay *et al*., Phys. Rev. B **58**, 12908 (1998).
[41] S. Winnerl, M. Orlita, P. Plochocka, P. Kossacki, M. Potemski, T. Winzer, E. Malic, A. Knorr, M. Sprinkle, C. Berger, W. A. de Heer, H. Schneider, and M. Helm, Phys. Rev. Lett. **107**, 237401 (2011).
[42] K. Seeger, *Semiconductor Physics* (Springer, Verlag, Wien, New York, 1973), p. 514.